

The role of spin-flipping terms in hadronic transitions of $\Upsilon(4S)$

Jorge Segovia^a, Francisco Fernández^a, and David R. Entem^a

^aGrupo de Física Nuclear and Instituto Universitario de Física Fundamental y Matemáticas (IUFFyM)
Universidad de Salamanca, E-37008 Salamanca, Spain

Abstract

Recent experimental data on the $\Upsilon(4S) \rightarrow \Upsilon(1S)\eta$ and $\Upsilon(4S) \rightarrow h_b(1P)\eta$ processes seem to contradict the naive expectation that hadronic transitions with spin-flipping terms should be suppressed with respect those without spin-flip. We analyze these transitions using the QCD Multipole Expansion (QCDME) approach and within a constituent quark model framework that has been applied successfully to the heavy-quark sectors during the last years. The QCDME formalism requires the computation of hybrid intermediate states which has been performed in a natural, parameter-free extension of our constituent quark model based on the Quark Confining String (QCS) scheme. We show that i) the M1-M1 contribution in the decay rate of the $\Upsilon(4S) \rightarrow \Upsilon(1S)\eta$ is important and its suppression until now is not justified; ii) the role played by the $L = 0$ hybrid states, which enter in the calculation of the M1-M1 contribution, explains the enhancement in the $\Upsilon(4S) \rightarrow \Upsilon(1S)\eta$ decay rate; and iii) the anomalously large decay rate of the $\Upsilon(4S) \rightarrow h_b(1P)\eta$ process has the same physical origin.

Keywords: Quantum Chromodynamics, potential models, heavy quarkonia, exotic mesons, hadronic decays of Quarkonia
PACS number: 12.38.-t, 12.39.Pn, 14.40.Pq, 14.40.Rt, 13.25.Gv

1. Introduction. Hadronic transitions are important decay modes for low-lying heavy quarkonium states. For instance, the first observed hadronic transition $\psi(2S) \rightarrow J/\psi\pi\pi$ [1] has a branching fraction reported by the Particle Data Group (PDG) of $(52.58 \pm 0.43)\%$ [2]. Moreover, during the last years, hadronic transitions between heavy quarkonia have led to an impressive series of discoveries which have helped the scientific community either to establish new conventional heavy quarkonium states, like the $h_b(1P)$ and $h_b(2P)$ observed in the two-pion decay of the $\Upsilon(5S)$ [3] state, or to extract relevant information of the so-called “XYZ” states, like in the cases of $X(3872)$ [4–6] and $X(4260)$ [7].

The general way of referring to an hadronic transition is [8]

$$\Phi_I \rightarrow \Phi_F + h, \quad (1)$$

where Φ_I and Φ_F stand, respectively, for the initial and final states of heavy quarkonium. The emitted light hadron(s), h , are kinematically dominated by single particle (π^0 , η , ω , ...) or two particle (2π , $2K$, ...) states. Since the typical mass difference between initial and final mesons, $m(\Phi_I) - m(\Phi_F)$, is around a few hundred MeV the momentum of the light hadron(s) is low. Therefore, certain nonperturbative approaches are needed for studying hadronic transitions and the standard one is the QCD Multipole Expansion (QCDME).

The QCDME has been studied by many authors [9–14], but Tung-Mow Yan was the first one to present a gauge-invariant formulation [15]. Many details about QCDME within the context of the Kuang-Yan model can be found in, for instance,

Refs. [16, 17]. The interested reader is also referred to the recent review [18] of Yu-Ping Kuang. Here, we want to highlight its basic feature: if the average size, a , of the heavy quark mesons involved in the hadronic transition is smaller than the wave length, $\lambda \sim 1/k$, of the radiated gluonic field such that $a/\lambda \sim ka < 1$, ka can be a good expansion parameter and thus one can expand the gluonic field in powers of ka .

The QCDME works well for hadronic transitions of heavy quarkonium states (at least for those which are located below or close to open-flavor threshold) and allows one to classify the transitions in a series of chromoelectric and chromomagnetic multiplets. The leading order term E1-E1 which goes in powers of v as $O(v^0 = (k/m_Q)^0)$ has $CP = ++$ and thus couples to 2π and $2K$ states. Higher-order terms couple as follows: E1-M1 in $O(v^1)$ with $CP = --$ couples to ω ; E1-M1, E1-E2 in $O(v^1)$ and M1-M1, E1-M2 in $O(v^2)$ with $CP = -+$ couples to both π^0 (isospin-breaking) and η ($SU(3)$ -breaking); and M1-M1, E1-E3, E2-E2 with $CP = ++$ are higher-order corrections to the E1-E1 terms.

The BaBar Collaboration has recently presented a systematic study of hadronic transitions between $\Upsilon(mS)$ ($m = 4, 3, 2$) and $\Upsilon(nS)$ ($n = 2, 1$) states, reporting the first observation of the $\Upsilon(4S) \rightarrow \eta\Upsilon(1S)$ [19]. Among their measurements, the most puzzling one is the following branching ratio

$$R_\eta[\Upsilon(4S)] = \frac{\Gamma(\Upsilon(4S) \rightarrow \Upsilon(1S)\eta)}{\Gamma(\Upsilon(4S) \rightarrow \Upsilon(1S)\pi^+\pi^-)} = 2.41 \pm 0.40 \pm 0.12, \quad (2)$$

which is strikingly large compared with those reported by PDG for the two vector bottomonium states that are below open-

Email addresses: segonza@usal.es (Jorge Segovia), fdz@usal.es (Francisco Fernández), entem@usal.es (and David R. Entem)

flavored threshold [2]:

$$\begin{aligned} R_\eta[\Upsilon(2S)] &= (1.63 \pm 0.23) \times 10^{-3}, \\ R_\eta[\Upsilon(3S)] &< 2.29 \times 10^{-3}. \end{aligned} \quad (3)$$

Note that similar figures were obtained in the work of the BaBar Collaboration [19].

Dimensional counting rules of QCDME establish that the branching ratio R_η scales as $O(v^2)$. The velocity, v , associated to the transition $\Upsilon(nS) \rightarrow \Upsilon(1S)\eta$ with $n = 2, 3$ and 4 is: 0.03, 0.16 and 0.22¹. Therefore, it seems feasible to expect branching ratios R_η of the order of $10^{-3} - 10^{-2}$.

The discrepancy between theory and experiment for the branching ratio $R_\eta[\Upsilon(4S)]$ has been attributed to neglect the effect of heavy-meson loops (see the related discussion in Ref. [8] and, for instance, Ref. [20]). A nonrelativistic effective field theory (NREFT) was introduced in Ref. [21] with the goal of determining the effect of heavy-meson loops with controlled uncertainty. The expansion parameter is the velocity of the heavy mesons in the intermediate state: v_{loop} . The NREFT determines that a typical hadronic transition via heavy-meson loop scales as

$$v_{\text{loop}}^3 / (v_{\text{loop}}^2)^2 \times \text{vertex factor}, \quad (4)$$

and, in the case of $R_\eta[\Upsilon(4S)]$, the vertex factor accounts for the transition between two S -wave bottomonia which takes place through a $B\bar{B}$ loop via a P -wave vertex. Therefore, the vertex factor scales as v_{loop}^2 and thus the heavy-meson loop contribution scales as order v_{loop} with

$$v_{\text{loop}} \sim \frac{\sqrt{[m[\Upsilon(4S)] - 2m[B]]}}{m[B]} = 6.26 \times 10^{-2}, \quad (5)$$

which is of the same order of magnitude than the naive expectation of QCDME for the $\Upsilon(4S) \rightarrow \Upsilon(1S)\eta$ decay. Therefore, heavy-meson loops cannot explain a factor $10^2 - 10^3$ in the branching ratio $R_\eta[\Upsilon(4S)]$.

Applying QCDME to hadronic transitions requires some phenomenological assumptions. The Hamiltonian for a heavy $Q\bar{Q}$ system in QCDME is given by [15]:

$$H_{\text{QCD}}^{\text{eff}} = H_{\text{QCD}}^{(0)} + H_{\text{QCD}}^{(1)} + H_{\text{QCD}}^{(2)}, \quad (6)$$

where $H_{\text{QCD}}^{(0)}$ represents the sum of the kinetic and potential energies of the heavy quarks, $H_{\text{QCD}}^{(1)}$ is related with the color charge of the $Q\bar{Q}$ system (which is zero for color singlets), and $H_{\text{QCD}}^{(2)}$ coupled color singlets to octet $Q\bar{Q}$ states. Therefore the hadronic transitions between eigenstates $|\Phi_I\rangle$ and $|\Phi_F\rangle$ of $H_{\text{QCD}}^{(0)}$ are at least second order in $H_{\text{QCD}}^{(2)}$ and the leading term is given by

$$\begin{aligned} \langle \Phi_F | h | H_{\text{QCD}}^{(2)} \frac{1}{E_I - H_{\text{QCD}}^{(0)} + i\partial_0 - H_{\text{QCD}}^{(1)}} H_{\text{QCD}}^{(2)} | \Phi_I \rangle &= \\ = \sum_{KL} \langle \Phi_F | h | H_{\text{QCD}}^{(2)} | KL \rangle \frac{1}{E_I - E_{KL}} \langle KL | H_{\text{QCD}}^{(2)} | \Phi_I \rangle & \end{aligned} \quad (7)$$

¹The velocity $v = k/m_Q$ is calculated using $k = \{[m[\Upsilon(nS)]^2 - (m[\Upsilon(1S)] - m[\eta])^2][m[\Upsilon(nS)]^2 - (m[\Upsilon(1S)] + m[\eta])^2]\} / 2m[\Upsilon(nS)]$ and the bottom-quark mass reported by PDG [2], 4.18 GeV.

where $|KL\rangle$ with associated energies E_{KL} are intermediate states after the emission of the first gluon and before the emission of the second gluon. They are states with a gluon and a color-octet $Q\bar{Q}$ and thus these states can be associated with the so-called hybrid mesons. A description of hybrid mesons is difficult from first principles of QCD and one is generally forced to use models. For instance, Kuang and Yan in Refs. [16–18] use the Buchmuller-Tye quark-confining string (QCS) model [22–24].

In Ref. [25] we pointed out that the particular location of hybrid mesons in the spectrum could explain big differences between hadronic transitions of the same type. This is due to the factor $1/(E_I - E_{KL})$ that appears in Eq. (7). This factor can be large for a particular $|\Phi_I\rangle$ state and leads to enhancements in the hadronic transition rates that are sensitive to the exact position of the intermediate states. The same observation was also done in Ref. [26].

In this work we shall calculate the branching ratios $R_\eta[\Upsilon(nS)]$ with $n = 2, 3, 4$ within the theoretical framework presented in Ref. [25]. This will allow us to disentangle the possible causes of having the $R_\eta[\Upsilon(4S)]$ much larger than those of the $\Upsilon(2S)$ and $\Upsilon(3S)$ mesons.

An important feature of the theoretical approach is that our model for hybrid mesons [25] is a parameter-free extension of a constituent quark model (CQM) [27] (see also references [28] and [29] for reviews) that describes quite well hadron phenomenology and hadronic reactions [30–32]. Furthermore, it has been recently applied to mesons containing heavy quarks with an extraordinary success, describing a wide range of physical observables which concern spectrum [33–35], strong reactions [36–38] and weak decays [39–41].

This manuscript is arranged as follows. In Sec. 2 we introduce the constituent quark model pointing out only those features which are relevant for this work. Section 3 is dedicated to explain the parameter-free extension of our quark model to describe hybrid mesons. Section 4 shows the QCDME formulation of the hadronic transitions highlighting its most relevant features. Our results are provided in Sec. 5. We finish giving some conclusions in Sec. 6.

2. Constituent quark model. The description of the meson spectra is based on the constituent quark model (CQM) proposed by Vijande *et al.* in Ref. [27]. One must solve the Schrödinger equation with a quark-antiquark potential whose main pieces are: i) the Goldstone-boson exchanges between constituent quarks which is a consequence of the dynamical chiral symmetry breaking in QCD, ii) the perturbative one-gluon fluctuations around the instanton vacuum, and iii) a phenomenological confining potential which reflects the empirical fact that quarks and gluons have never been seen as isolated particles. Note that in the heavy quark sector chiral symmetry is explicitly broken and Goldstone-boson exchanges do not appear.

Further details about the CQM and the fine-tuned model parameters can be found in Refs. [27, 33, 44]. Here we want to explain in more detail our confinement potential because its screened linear shape is a particular feature of the model. It is well known that multigluon exchanges produce an attractive

State	Mass (CQM) (MeV)	Mass (Cornell) (MeV)	Mass (Exp.) (MeV)	$\langle r^2 \rangle^{1/2}$ (CQM) (fm)	$\langle r^2 \rangle^{1/2}$ (Cornell) (fm)
$\Upsilon(1S)$	9502	9460	9460.30 ± 0.26	0.24	0.20
$\Upsilon(2S)$	10015	10050	10023.26 ± 0.31	0.50	0.48
$\Upsilon(3S)$	10349	10400	10355.2 ± 0.5	0.74	0.72
$\Upsilon(4S)$	10607	10670	10579.4 ± 1.2	0.96	0.92

Table 1: Masses, in MeV, and radius, in fm, of the S -wave vector bottomonium states up to $n = 4$ predicted by our CQM and by the Cornell model [42, 43]. Experimental masses are taken from PDG [2]. The experimental value of the mass of the $\Upsilon(1S)$ has been used to fit the free constant that appears in the Cornell potential.

linearly rising potential proportional to the distance between infinite heavy quarks. However, sea quarks are also important ingredients of the strong interaction dynamics that contribute to the screening of the rising potential at low momenta and eventually to the breaking of the quark-antiquark binding string [45]. Our model try to mimic this behavior using the following confining potential

$$V_{\text{CON}}(\vec{r}) = [-a_c(1 - e^{-\mu_c r}) + \Delta](\vec{\lambda}_q^c \cdot \vec{\lambda}_{\bar{q}}^c), \quad (8)$$

where a_c and μ_c are parameters, r is the interquark distance and $\vec{\lambda}_{q(\bar{q})}^c$ are $SU(3)$ color matrices. At short distances this potential presents a linear behavior with an effective confinement strength $\sigma = -a_c \mu_c (\vec{\lambda}_q^c \cdot \vec{\lambda}_{\bar{q}}^c)$, while it becomes constant at large distances showing a threshold defined by $V_{\text{thr}} = [-a_c + \Delta](\vec{\lambda}_q^c \cdot \vec{\lambda}_{\bar{q}}^c)$. No $q\bar{q}$ bound states can be found for energies higher than this threshold.

The screened linear potential is a key feature to reproduce the degeneracy pattern observed for the higher excited states of light mesons [44]. As we assume that confining interaction is flavor independent, this affects also to the different quark sectors and, in particular, the bottomonium spectrum. Table 1 shows the S -wave vector bottomonium states up to $n = 4$ predicted by our quark model. We compare masses with the standard Cornell model [42, 43] and the experimental data reported by PDG [2]. Both models reproduce quite well the experimental data. In the Cornell model the ground state is fitted to the experimental figure while in our case the model parameters are fitted to all meson sectors. One can see that our quark model is able to reproduce in better agreement the excited states which is a particular feature of the screening of the linear confinement potential. Since the size of the mesons involved in the hadronic transitions are important in QCDME in order to determine if the expansion parameter is sufficiently small, we also show in Table 1 the typical radius of the bottomonium states and compare with those predicted by the Cornell model. Both models predict pretty similar results. The size of these mesons are in the order of 10^{-1} fm and thus for the hadronic transitions in which we are interested, where the gluon momentum is in the order of few hundred MeV, QCDME is expected to work reasonably well.

3. A model for hybrids. From the generic properties of QCD, we might expect to have states in which the gluonic field itself is excited and carries J^{PC} quantum numbers. A bound-state is called glueball when any valence quark content is absent, the addition of a constituent quark-antiquark pair to an excited

gluonic field gives rise to what is called a hybrid meson. The gluonic quantum numbers couple to those of the $q\bar{q}$ pair. This coupling may give rise to so-called exotic J^{PC} mesons, but also can produce hybrid mesons with natural quantum numbers. We are interested on describing the last ones because, as pointed out in Eq. (7), they are involved in the calculation of hadronic transitions within the QCDME approach.

Ab-initio QCD calculations of the hybrid (even conventional) bottomonium states are particularly difficult because the large mass of the b -quark. Therefore, the only way up to now to describe hybrid mesons in the bottomonium sector is through models. An extension of the quark model described above to include hybrid states has been presented in Ref. [25]. This extension is inspired on the Buchmuller-Tye quark-confining string (QCS) model [22–24] which assumes that the meson is composed of a quark and antiquark linked by an appropriate color electric flux line: the string. Gluon excitation effects are described by the vibration of the string. These vibrational modes provide new states beyond the naive meson picture and are interpreted as hybrid mesons.

The coupled equations that describe the dynamics of the string, quark and antiquark sectors are highly nonlinear so that there is no hope of solving them completely. Then, to introduce the vibrational modes, we use the following approximation scheme. First, we solve the string Hamiltonian via the Bohr-Oppenheimer method to obtain the vibrational energies as a function of the interquark distance [23]

$$V_n(r) = \sigma(r)r \left\{ 1 + \frac{2n\pi}{\sigma(r)[(r-2d)^2 + 4d^2]} \right\}^{1/2}. \quad (9)$$

Note that $n = 0$ gives $V_0(r) = \sigma(r)r$ where $\sigma(r) = (16/3)a_c [(1 - e^{-\mu_c r})/r]$ attending to Eq. (8). The parameter d is the correction due to the finite heavy quark mass

$$d(m_Q, r, \sigma, n) = \frac{\sigma r^2 \alpha_n}{4(2m_Q + \sigma r \alpha_n)}, \quad (10)$$

where α_n is related with the shape of the vibrating string and can take the values $1 \leq \alpha_n \leq \sqrt{2}$.

Second, the vibrational potential is inserted into the meson equation as an effective potential

$$V_{\text{hyb}}(r) = V_{\text{OGE}}(r) + V_{\text{CON}}(r) + [V_n(r) - \sigma(r)r], \quad (11)$$

where $V_{\text{OGE}}(r) + V_{\text{CON}}(r)$ is the naive quark-antiquark potential in the heavy quark sector and $V_n(r)$ is the vibrational potential

K/L	0	1
1	10571	10785
2	10857	10999
3	11063	11175
4	11232	11325
5	11374	11452
6	11496	11562
7	11600	11657
8	11690	11738
9	11766	11807
10	11831	11866
11	11885	11913
12	11927	-
$V_{\text{thr}} = 11943$		

Table 2: Masses, in MeV, of those hybrid states in the bottomonium sector that participate in the hadronic transitions calculated in this paper. K and L are the hybrid meson quantum numbers as appear in Eq. (7).

calculated above. We must subtract the term $\sigma(r)r$ because it appears twice, one in $V_{\text{CON}}(r)$ and the other one in $V_n(r)$.

We have arrived to a description of the hybrid mesons in the heavy quark sector that does not include new parameters besides those of the original quark model². In that sense, our calculation of the hybrid states is parameter-free. Another important feature of our hybrid model is that, just like the naive quark model, the hybrid potential has a threshold from which no more states can be found and so we have a finite number of hybrid states in the spectrum.

Table 2 shows our theoretical prediction for those hybrid states in the bottomonium sector that will participate in the hadronic transitions in which we are interested. They are classified by the quantum numbers $|KL\rangle$ as appear in Eq. (7). It is important to realize here that we predict a hybrid meson with quantum numbers $|KL\rangle = |10\rangle$ which is very close in mass, 10571 MeV, to the $\Upsilon(4S)$ state, 10607 MeV. As we will see later, this feature have important consequences in the calculation of the $\Upsilon(4S)$ hadronic decay rates.

4. Hadronic decay rates. A detailed description of the computation of the decay rates in the single-channel approach of QCDME for the hadronic transitions:

$$\begin{aligned} {}^3S_1 &\rightarrow {}^3S_1 + \pi\pi, \\ {}^3S_1 &\rightarrow {}^3S_1 + \eta, \end{aligned} \quad (12)$$

can be found in Ref. [16]. See also Ref. [18] for an updated review and Ref. [25] for a calculation of two-pion spin-nonflip hadronic transitions within our model.

The most relevant feature of this formalism is that the hadronic transition amplitude always splits into two factors (see Fig. 1). The first one concerns the multipole gluon emission (MGE) from the heavy quarks and the second one is

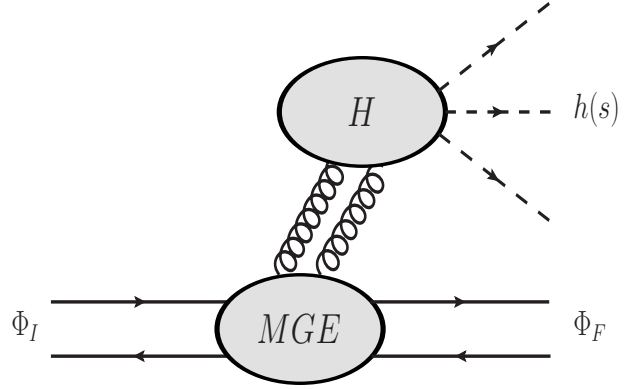


Figure 1: A hadronic transition as a two-step process: (1) emission of gluons from heavy quarks (MGE), and (2) the conversion of gluons into light hadrons (H).

an hadronization (H) process describing the conversion of the emitted gluons into light hadron(s).

The MGE vertex involves the wave functions and energies of the initial and final quarkonium states as well as those of the intermediate hybrid mesons. All these quantities are calculated within our model and enter in the hadronic transition rate with integrals of the type:

$$\begin{aligned} f_{IF}^{LP_I P_F} &= \sum_K \frac{1}{M_I - M_{KL}} \left[\int dr r^{2+P_F} R_F(r) R_{KL}(r) \right] \times \\ &\times \left[\int dr' r'^{2+P_I} R_{KL}(r') R_I(r') \right], \end{aligned} \quad (13)$$

where $R_I(r)$ and $R_F(r)$ are, respectively, the radial wave functions of the initial and final states. $R_{KL}(r)$ is the radial wave function of the intermediate vibrational states $|KL\rangle$. The mass of the decaying meson is M_I , whereas the ones corresponding to the hybrid states are M_{KL} .

The H vertex is at the scale of the light hadron(s) and is independent of the properties of the heavy quarkonia and hybrid states. There are two ways of calculating the matrix elements associated with the H factor: (H1) using PCAC and soft pion techniques [15, 46] or (H2) using a duality argument between the physical light hadron final state and the associated two-gluon final state [16]. Both approaches involve unknown coefficients. However, the difference between the two is that the H1-approach needs, at least, one coefficient for each multipole matrix element (we will denote these coefficients by C_i 's), whereas in the H2-approach all these matrix elements are written in function of only two parameters (g_E and g_M). For clarity, when the gluons are converted into two pions ($h = \pi_1 + \pi_2$) the coefficients of both approaches are related as follows:

$$\begin{aligned} \frac{g_E^2}{6} \langle \pi_1 \pi_2 | E_i^a E_j^a | 0 \rangle &= \frac{1}{\sqrt{(2\omega_1)(2\omega_2)}} \left[C_1 \delta_{ij} q_1^\mu q_{2\mu} \right. \\ &\left. + C_2 \left(q_{1i} q_{2j} + q_{1j} q_{2i} - \frac{2}{3} \delta_{ij} q_1^\mu q_{2\mu} \right) \right], \end{aligned} \quad (14)$$

whereas in the case in which the gluons make up an η -meson

²The variation of the parameter α_n within its range $[1, \sqrt{2}]$ modifies around 30 MeV the mass of a hybrid state in the bottomonium sector, we have chosen the mean value $\alpha_n = \sqrt{1.5}$.

Process		H1-approach	H2-approach	Experiment [2]
$\Upsilon(3S) \rightarrow \Upsilon(1S)\pi^+\pi^-$	(keV)	1.18	0.80	0.89 ± 0.08
$\Upsilon(3S) \rightarrow \Upsilon(1S)\eta$	(keV)	7.59×10^{-3}	20.58×10^{-3}	$< 2.03 \times 10^{-3}$
$R_\eta[\Upsilon(3S)]$		6.43×10^{-3}	25.7×10^{-3}	$< 2.29 \times 10^{-3}$
$\Upsilon(4S) \rightarrow \Upsilon(1S)\pi^+\pi^-$	(keV)	4.01	2.54	1.66 ± 0.24
$\Upsilon(4S) \rightarrow \Upsilon(1S)\eta$	(keV)	12.60×10^{-3}	6.05	4.02 ± 0.76
$R_\eta[\Upsilon(4S)]$		3.14×10^{-3}	2.38	2.42 ± 0.39

Table 3: The decay widths, in keV, of the $\Upsilon(3S)$ and $\Upsilon(4S)$ hadronic transitions into $\Upsilon(1S)\pi^+\pi^-$ and $\Upsilon(1S)\eta$ channels. The ratio $R_\eta[\Upsilon(nS)] = \Gamma(\Upsilon(nS) \rightarrow \Upsilon(1S)\eta)/\Gamma(\Upsilon(nS) \rightarrow \Upsilon(1S)\pi^+\pi^-)$ is also given. The experimental data is taken from PDG [2].

($h = \eta$) we have:

$$\frac{g_E g_M}{6} \langle \eta | E_i^a \partial_i B_j^a | 0 \rangle = i(2\pi)^{3/2} C_3 q_j. \quad (15)$$

A further comment is necessary here. The leading multipoles of an η transition between spin-triplet S -wave states are M1-M1 and E1-M2. Therefore, the matrix element is given schematically by

$$\mathcal{M}(^3S_1 \rightarrow ^3S_1 + \eta) = \mathcal{M}_{M1M1} + \mathcal{M}_{E1M2}. \quad (16)$$

The H1-approach only considers the E1-M2 multipole gluon emission because it is difficult to find a relation to fix the M1-M1 corresponding parameter, whereas the H2-approach considers a priori both of them. There is no reason to neglect the M1-M1 contribution and this will be a key feature in order to explain the large value of the $\Upsilon(4S) \rightarrow \Upsilon(1S)\eta$ decay rate.

For completeness and because it is important for the discussion in the next section, we show here the expressions in both approaches for the $^3S_1 \rightarrow ^3S_1 + \pi\pi$ transition:

$$\Gamma_{\pi\pi}^{H1} = G C_1^2 |f_{IF}^{111}|^2, \quad (17)$$

$$\Gamma_{\pi\pi}^{H2} = \left(\frac{g_E^2}{2} \right)^2 \frac{(M_I - M_F)^7}{1890\pi^3} |f_{IF}^{111}|^2, \quad (18)$$

and for the $^3S_1 \rightarrow ^3S_1 + \eta$ transition:

$$\Gamma_\eta^{H1} = \frac{8\pi^2}{27} \frac{M_F C_3^2}{M_I m_Q^2} |\vec{q}|^3 |f_{IF}^{111}|^2, \quad (19)$$

$$\begin{aligned} \Gamma_\eta^{H2} &= \left(\frac{g_M^2}{3m_Q^2} \right)^2 \frac{1}{12\pi^3} \frac{(M_I - M_F)^7}{140} |f_{IF}^{000}|^2 + \\ &+ \left(\frac{g_E g_M}{3m_Q} \right)^2 \frac{1}{12\pi^3} \frac{(M_I - M_F)^9}{6804} |f_{IF}^{111}|^2, \end{aligned} \quad (20)$$

where the factor G is a phase-space integral defined in Eq. (2.4) of Ref. [16], \vec{q} is the momentum of η and $f_{IF}^{LP_i P_F}$ has been defined in Eq. (13).

5. Results. The transitions $\Upsilon(2S) \rightarrow \Upsilon(1S)\pi^+\pi^-$ and $\Upsilon(2S) \rightarrow \Upsilon(1S)\eta$ help us to fix our unknown coefficients. The experimental data [2]

$$\Gamma(\Upsilon(2S) \rightarrow \Upsilon(1S)\pi^+\pi^-) = 5.71 \pm 0.48 \text{ keV}, \quad (21)$$

fixes the constant C_1 in the H1-approach. Once we get C_1 the coefficient g_E is determined through Eqs. (17) and (18). Our

values of these two constants are³:

$$\begin{aligned} C_1 &= 7.69 \times 10^{-3}, \\ g_E &= 2.17, \end{aligned} \quad (22)$$

which compare well, for instance, with the ones used in the Kuang-Yan model [16]: $C_1^{KY} = 7.86 \times 10^{-3}$ and $g_E^{KY} = 2.61$.

Now, the constants C_3 and g_M are fixed to the experimental figure of the $\Upsilon(2S) \rightarrow \Upsilon(1S)\eta$ decay rate [2]

$$\Gamma(\Upsilon(2S) \rightarrow \Upsilon(1S)\eta) = (9.27 \pm 1.49) \times 10^{-3} \text{ keV}, \quad (23)$$

and we obtain:

$$\begin{aligned} C_3 &= 2.96 \times 10^{-6} \\ g_M &= 5.70 \end{aligned} \quad (24)$$

which are also compatible with the values reported in Ref. [16] using the Kuang-Yan model.

Table 3 shows our theoretical results for the hadronic transitions of the $\Upsilon(3S)$ and $\Upsilon(4S)$ into $\Upsilon(1S)\pi^+\pi^-$ and $\Upsilon(1S)\eta$ channels. The ratio $R_\eta[\Upsilon(nS)] = \Gamma(\Upsilon(nS) \rightarrow \Upsilon(1S)\eta)/\Gamma(\Upsilon(nS) \rightarrow \Upsilon(1S)\pi^+\pi^-)$ for $n = 3, 4$ is also given. The most remarkable feature of this table is the result we obtain for the $R_\eta[\Upsilon(4S)]$. While the ratio predicted within the H1-approach is of the order of 10^{-3} , the calculated value using the H2-approach is of the order of unity and agrees nicely with the experimental measurement.

Our result has a natural explanation. The rate of the $\Upsilon(4S)$ hadronic decay into the $\Upsilon(1S)\eta$ final state has two terms. One is a M1-M1 contribution which involves the hybrid states of $L = 0$ through the term f_{IF}^{000} (see Eq. (20)), whereas the other one is a E1-M2 contribution which involves the $L = 1$ hybrid mesons through the term f_{IF}^{111} (see again Eq. (20)). Different hybrid intermediate states enter in the calculation of the M1-M1 and E1-M2 terms. The M1-M1 contribution has been usually neglected in the H1-approach despite dimensional counting rules determine that M1-M1 and E1-M2 terms are of the same order of magnitude. Our result indicates that the M1-M1 contribution to the hadronic decay rate can be (very) important because the role played by the $L = 0$ hybrid spectrum.

³Note that the value reported here for C_1 differs to the one used in our previous work [25]: 9.69×10^{-3} , we decided to fit here the bottomonium case instead of the charmonium one in order to eliminate sources of uncertainty. One can realize that the difference is small ($\sim 10\%$) and it is not going to change our conclusions.

The $L = 0$ hybrid spectrum should be lower in energy than the $L = 1$ spectrum. This is a general feature, but a model-dependent result is given in Table 2. The masses predicted by our model for the ground states of hybrid mesons with $L = 0$ and $L = 1$ are 10.6 GeV and 10.8 GeV, respectively. The $\Upsilon(4S)$ is very close in mass to the ground state of hybrid mesons with $L = 0$, and thus the mass denominator $M_I - M_{KL}$ in Eq. (13) leads to a large enhancement of the $\Upsilon(4S) \rightarrow \Upsilon(1S)\eta$ decay rate through the M1-M1 term. The mass splitting between the $\Upsilon(4S)$ and the ground state of hybrid mesons with $L = 1$ is around 0.2 GeV, which is enough to predict $\Gamma(\Upsilon(4S) \rightarrow \Upsilon(1S)\eta) = 12.92 \times 10^{-3}$ keV when we consider only the E1-M2 term. Note that this number is very close to the one obtained using the H1-approach.

Table 3 also shows the $\Upsilon(3S) \rightarrow \Upsilon(1S)\pi^+\pi^-$ and $\Upsilon(3S) \rightarrow \Upsilon(1S)\eta$ decay rates using H1- and H2-approaches. The theoretical widths of the $\Upsilon(3S) \rightarrow \Upsilon(1S)\pi^+\pi^-$ process are compatible with the experimental data, being that of the H2-approach in better agreement with experiment. Only an upper limit of the decay rate for the $\Upsilon(3S) \rightarrow \Upsilon(1S)\eta$ process is reported by PDG [2]. Our predicted values are higher than this upper limit by a factor ~ 3 for the H1-approach and a factor ~ 10 for the H2-approach. The factor is larger in the H2-approach because there are two contributions to the decay rate, M1-M1 and E1-M2. Taking into account only the E1-M2 contribution we obtain $\Gamma(\Upsilon(3S) \rightarrow \Upsilon(1S)\eta) = 2.59 \times 10^{-3}$ which is compatible with the experimental upper limit but still slightly higher. We encourage experimentalists to determine this decay rate with better precision in order to clarify the situation.

Finally, the PDG [2] does not provide any experimental result on the η transitions among spin-triplet and spin-singlet states. These transitions are an alternative way of determining the properties of the h_b states beyond the hadronic isospin suppressed transition $\Upsilon(nS) \rightarrow h_b(1P)\pi^0$. Moreover, the study of them is motivated by the extraordinary success of finding spin-singlet charmonium and bottomonium states in double pion decays of heavy vector quarkonium states.

The Belle Collaboration has recently measured for the first time the branching fraction $\mathcal{B}(\Upsilon(4S) \rightarrow h_b(1P)\eta) = (2.18 \pm 0.11 \pm 0.18) \times 10^{-3}$ [47]. This branching fraction provides a decay rate of (44.69 ± 6.95) keV when combined with the total decay width [2] of the $\Upsilon(4S)$ state. This value is again anomalously large because one would expect a suppression of the transitions with spin flipping terms.

The expression for the decay rate of the $\Upsilon(nS) \rightarrow h_b(mS)\eta$ hadronic transition can be extracted from Eq. (56) of Ref. [18] and reads as

$$\Gamma(\Upsilon(nS) \rightarrow h_b(mP)\eta) = \frac{\pi}{1144m_Q^2} \frac{g_M^2}{g_E^2} \frac{M_F|\vec{q}|}{M_I} \times \left(\frac{4\pi}{\sqrt{6}} f_\pi m_\eta^2 \right)^2 |f_{IF}^{001} + f_{IF}^{110}|^2. \quad (25)$$

As one can see in Eq. (25), both $L = 0$ and $L = 1$ hybrid states are involved in this kind of transitions through the factors f_{IF}^{001} and f_{IF}^{110} , respectively. We predict

$$\Gamma(\Upsilon(4S) \rightarrow h_b(1P)\eta) = 37.89 \text{ keV}, \quad (26)$$

which is in good agreement with the experimental figure. The enhancement of this decay width has the same physical origin than the one found in the decay rate of the $\Upsilon(4S) \rightarrow \Upsilon(1S)\eta$ process: we are predicting a hybrid bottomonium meson which is very close in mass to the $\Upsilon(4S)$. The location of the hybrid mesons in the spectrum is a model-dependent result but our prediction seems to explain two uncorrelated processes, even a third one considering our results in Ref. [25]. It is worth to remark that the construction of our hybrid model does not add any new parameter of a quark model which explains a very large number of hadron phenomenology. In a more conservative way, if there is any truth in the QCDME approach, large enhancements in certain hadronic transition rates could point out the presence of hybrid mesons.

6. Conclusions. Recent experiments on the $\Upsilon(4S) \rightarrow \Upsilon(1S)\eta$ and $\Upsilon(4S) \rightarrow h_b(1P)\eta$ transitions have pointed out their anomalously large decay rates. This seem to contradict the naive expectation that hadronic transitions with spin flipping terms should be suppressed with respect those that do not have these terms.

We have studied these transitions within the theoretical framework of a constituent quark model that has been applied successfully to a wide range of hadron observables. In particular, this model has been used in the last few years to study spectra, strong reactions and weak decays in the heavy quark sectors. Therefore, we consider that the quark model parameters are very well constrained for the study of hadronic transitions between heavy quarkonia.

The calculation of the hadronic decay rates has been performed using the QCDME approach. This formalism requires the computation of a hybrid meson spectrum. We have calculated the hybrid states using a natural, parameter-free extension of our quark model based on the Quark Confining String scheme.

The rate of the $\Upsilon(4S) \rightarrow \Upsilon(1S)\eta$ hadronic decay has two leading multipole gluon emission terms: M1-M1 and E1-M2. Until now, the M1-M1 contribution has been neglected. We have shown here that the hybrid meson spectrum involved in the calculation of the M1-M1 and E1-M2 contributions is different. The M1-M1 contribution involves the hybrid states of $L = 0$, whereas the E1-M2 contribution involves the $L = 1$ hybrid mesons. The $\Upsilon(4S)$ is very close in mass to our predicted ground state of hybrid mesons with $L = 0$, and this leads to a large enhancement of the $\Upsilon(4S) \rightarrow \Upsilon(1S)\eta$ decay rate through the M1-M1 term.

The anomalously large $\Upsilon(4S) \rightarrow \Upsilon(1S)\eta$ decay rate has been usually attributed to the effect of heavy-meson loops. Since the $\Upsilon(4S)$ is so close to the $B\bar{B}$ threshold, the dimensional counting rules of a NREFT establish that the meson-loop effect is very small and cannot explain factors of $10^2 - 10^3$.

We have seen that the surprisingly large enhancement observed by the Belle Collaboration in the decay $\Upsilon(4S) \rightarrow h_b(1P)\eta$ has the same physical origin than the one found in the decay $\Upsilon(4S) \rightarrow \Upsilon(1S)\eta$: we are predicting a hybrid bottomonium meson very close in mass to the $\Upsilon(4S)$. The location of the hybrid mesons in the spectrum is a model-dependent result

but our prediction seems to explain two uncorrelated processes, even a third one considering our results in Ref. [25].

Finally, we would like to emphasize that if there is any truth in the QCDME approach, large enhancements in certain hadronic transition rates could point out the presence of hybrid mesons.

Acknowledgements. This work has been partially funded by Ministerio de Ciencia y Tecnología under Contract no. FPA2013-47443-C2-2-P, by the European Community-Research Infrastructure Integrating Activity “Study of Strongly Interacting Matter” (HadronPhysics3 Grant no. 283286) and by the Spanish Ingenio-Consolider 2010 Program CPAN (CSD2007-00042). J. Segovia acknowledges financial support from a postdoctoral IUFFyM contract of the Universidad de Salamanca, Spain.

References.

References

- [1] G. Abrams et al., Phys. Rev. Lett. **34**, 1181 (1975).
 [2] K. Olive et al. (Particle Data Group), Chin. Phys. **C38**, 090001 (2014).
 [3] I. Adachi et al. (Belle), Phys. Rev. Lett. **108**, 032001 (2012).
 [4] B. Aubert et al. (BaBar), Phys. Rev. Lett. **93**, 041801 (2004).
 [5] B. Aubert et al. (BaBar), Phys. Rev. **D77**, 111101 (2008).
 [6] P. del Amo Sanchez et al. (BaBar), Phys. Rev. **D82**, 011101 (2010).
 [7] J. Lees et al. (BaBar), Phys. Rev. **D86**, 051102 (2012).
 [8] N. Brambilla, S. Eidelman, B. Heltsley, R. Vogt, G. Bodwin, et al., Eur. Phys. J. **C71**, 1534 (2011).
 [9] K. Gottfried, Phys. Rev. Lett. **40**, 598 (1978).
 [10] G. Bhanot, W. Fischler, and S. Rudaz, Nucl. Phys. **B155**, 208 (1979).
 [11] M. E. Peskin, Nucl. Phys. **B156**, 365 (1979).
 [12] G. Bhanot and M. E. Peskin, Nucl. Phys. **B156**, 391 (1979).
 [13] M. Voloshin, Nucl. Phys. **B154**, 365 (1979).
 [14] M. B. Voloshin and V. I. Zakharov, Phys. Rev. Lett. **45**, 688 (1980).
 [15] T.-M. Yan, Phys. Rev. **D22**, 1652 (1980).
 [16] Y.-P. Kuang and T.-M. Yan, Phys. Rev. **D24**, 2874 (1981).
 [17] Y.-P. Kuang, Y.-P. Yi, and B. Fu, Phys. Rev. **D42**, 2300 (1990).
 [18] Y.-P. Kuang, Front. Phys. China **1**, 19 (2006).
 [19] B. Aubert et al. (BaBar), Phys. Rev. **D78**, 112002 (2008).
 [20] F.-K. Guo, C. Hanhart, G. Li, U.-G. Meissner, and Q. Zhao, Phys. Rev. **D82**, 034025 (2010).
 [21] F.-K. Guo, C. Hanhart, and U.-G. Meissner, Phys. Rev. Lett. **103**, 082003 (2009).
 [22] S. Tye, Phys. Rev. **D13**, 3416 (1976).
 [23] R. Giles and S. Tye, Phys. Rev. **D16**, 1079 (1977).
 [24] W. Buchmuller and S. Tye, Phys. Rev. **D24**, 132 (1981).
 [25] J. Segovia, D. R. Entem, and F. Fernandez, Phys. Rev. **D91**, 014002 (2015).
 [26] H.-W. Ke, J. Tang, X.-Q. Hao, and X.-Q. Li, Phys. Rev. **D76**, 074035 (2007).
 [27] J. Vijande, F. Fernandez, and A. Valcarce, J. Phys. **G31**, 481 (2005).
 [28] A. Valcarce, H. Garcilazo, F. Fernandez, and P. Gonzalez, Rept. Prog. Phys. **68**, 965 (2005).
 [29] J. Segovia, D. R. Entem, F. Fernandez, and E. Hernandez, Int. J. Mod. Phys. **E22**, 1330026 (2013).
 [30] F. Fernandez, A. Valcarce, P. Gonzalez, and V. Vento, Phys. Lett. **B287**, 35 (1992).
 [31] H. Garcilazo, A. Valcarce, and F. Fernandez, Phys. Rev. **C63**, 035207 (2001), *ibid.* Phys. Rev. C64, 058201 (2001).
 [32] J. Vijande, H. Garcilazo, A. Valcarce, and F. Fernandez, Phys. Rev. **D70**, 054022 (2004).
 [33] J. Segovia, A. Yasser, D. R. Entem, and F. Fernandez, Phys. Rev. **D78**, 114033 (2008).
 [34] J. Segovia, A. Yasser, D. R. Entem, and F. Fernandez, Phys. Rev. **D80**, 054017 (2009).
 [35] J. Segovia, D. R. Entem, and F. Fernandez, Phys. Rev. **D91**, 094020 (2015).
 [36] J. Segovia, D. R. Entem, and F. Fernandez, Phys. Rev. **D83**, 114018 (2011).
 [37] J. Segovia, D. R. Entem, and F. Fernandez, Phys. Lett. **B715**, 322 (2012).
 [38] J. Segovia, D. R. Entem, and F. Fernandez, Nucl. Phys. **A915**, 125 (2013).
 [39] J. Segovia, C. Albertus, D. R. Entem, F. Fernandez, E. Hernandez, et al., Phys. Rev. **D84**, 094029 (2011).
 [40] J. Segovia, C. Albertus, E. Hernandez, F. Fernandez, and D. R. Entem, Phys. Rev. **D86**, 014010 (2012).
 [41] J. Segovia, E. Hernandez, F. Fernandez, and D. R. Entem, Phys. Rev. **D87**, 114009 (2013).
 [42] E. Eichten, K. Gottfried, T. Kinoshita, K. Lane, and T.-M. Yan, Phys. Rev. **D17**, 3090 (1978).
 [43] E. Eichten, K. Gottfried, T. Kinoshita, K. Lane, and T.-M. Yan, Phys. Rev. **D21**, 203 (1980).
 [44] J. Segovia, D. Entem, and F. Fernandez, Phys. Lett. **B662**, 33 (2008).
 [45] G. S. Bali, H. Neff, T. Duessel, T. Lippert, and K. Schilling (SESAM), Phys. Rev. **D71**, 114513 (2005).
 [46] L. S. Brown and R. N. Cahn, Phys. Rev. Lett. **35**, 1 (1975).
 [47] U. Tamponi et al. (The Belle Collaboration) (2015), arXiv:hep-ex/1506.08914.